Magnetization densities in UCoAl studied by polarized neutron diffraction

P. Javorský* and V. Sechovský
Department of Electronic Structures, Charles University, Ke Karlovu 5, 12116 Prague 2, The Czech Republic

J. Schweizer and F. Bourdarot
CEA, Département de Recherche Fondamentale sur la Matière Condensée SPSMS/MDN, Centre d'Etudes Nucléaires de Grenoble, 85 X, 38054 Grenoble Cedex 9, France

E. Lelièvre-Berna
Institut Laue Langevin, 6 rue Jules Horowitz, 38042 Grenoble Cedex 9, France

A. V. Andreev
Institute of Physics, Academy of Sciences of the Czech Republic, Na Slovance 2, 182 21 Prague 8, The Czech Republic

Y. Shiokawa
Institute for Material Research, Tohoku University, Katahira 2-1-1, Aoba-ku, Sendai 980-8577, Japan
(Received 24 August 2000; published 23 January 2001)

UCoAl crystallizes in the ZrNiAl-type hexagonal structure, exhibits a paramagnetic ground state, but a metamagnetic transition to a ferromagnetic state with uranium magnetic moments parallel to the *c* axis occurs at low temperatures when a field of 1 T is applied in this direction. We present the results of a polarized neutron experiment on a UCoAl single crystal. Experimental data have been analyzed by a maximum entropy method and within an atomic model. The main magnetic contribution originates from the uranium atoms. The ratio μ_L/μ_S between the orbital and spin moment is slightly reduced in comparison to the uranium free ion value and remains nearly unchanged between 1 and 8 T. Induced magnetic moments of nearly same magnitude and similar field dependence are observed on the two cobalt sites. An additional magnetization density is observed around the aluminum positions. The results are discussed in context of former studies on isostructural U*TX* compounds.

DOI: 10.1103/PhysRevB.63.064423 PACS number(s): 75.25.+z, 75.30.−m, 75.30.Gw

I. INTRODUCTION

The magnetic and other electronic properties of uranium intermetallic compounds are affected by the delocalization of the $5f$ electrons due to the overlap between $5f$-electron wave functions of neighboring uranium atoms and by the hybridization between the uranium $5f$ states and the electron states of other neighboring atoms. Both mechanisms depend strongly on the crystalline surrounding of the uranium atoms. Comparison of a large group of isostructural compounds can be thus essential for more general understanding of the physics of uranium intermetallics. The U*TX* (*T* is a late transition metal, *X* is a *p* metal) compounds crystallizing in the hexagonal ZrNiAl-type structure constitute such a system. Depending on *X* and *T* components, the magnetic properties of these compounds are ranging from Pauli paramagnetism to spin fluctuation effects, metamagnetism, and magnetic ordering with stable uranium magnetic moments.[1]

An important characteristic of most of these compounds is a strong uniaxial magnetocrystalline anisotropy with the easy magnetization axis parallel to the hexagonal *c* axis. Possible origin of this magnetic anisotropy was discussed in case of URhAl and URuAl (Refs. 2 and 3) on the basis of polarized neutron-diffraction experiments. Both compounds exhibit similar magnetic anisotropy although their magnetic ground states are different: URhAl orders ferromagnetically with a considerable uranium moment $(0.94\mu_B)$,[2] while URuAl is paramagnetic. The polarized neutron-diffraction experiments revealed a strongly anisotropic hybridization between the uranium $5f$ states and the $4d$ states of Rh or Ru. Relatively large magnetic moment induced by hybridization has been observed on the T_1 (T=Rh or Ru) site, which lies in the (001) plane together with the U atoms (see Fig. 1), while the T_2 site, which is at the same distance from uranium but out of this plane, does not show such induced moment. The anisotropic hybridization has been proposed as a possible source of the large bulk magnetic anisotropy. Recent polarized neutron diffraction on UNiAl and UNiGa showed that for these two compounds a larger magnetic moment is induced on the T_2 site.[4] In the case of UCoAl, comparable moments on both cobalt sites have been reported.[5,6]

UCoAl became one of the most intensively studied U*TX* compounds.[1] The ground state of UCoAl is considered to be paramagnetic. When a magnetic field of $\approx$1 T is applied along the *c* axis of UCoAl below 13 K, a metamagnetic transition to a high-field ferromagnetic state with uranium magnetic moments parallel to the *c* axis is observed.[7] The magnetization along the *c* axis does not saturate above the metamagnetic transition but shows a strong, almost linear increase with increasing field ($M_{1T}=0.334\mu_B$, $M_{8T}=0.445\mu_B$). Here, we present a more precise polarized neutron-diffraction study of this compound performed on a single crystal of well defined stoichiometry 1:1:1. We concentrate on two points: (i) describe the magnetization distri-

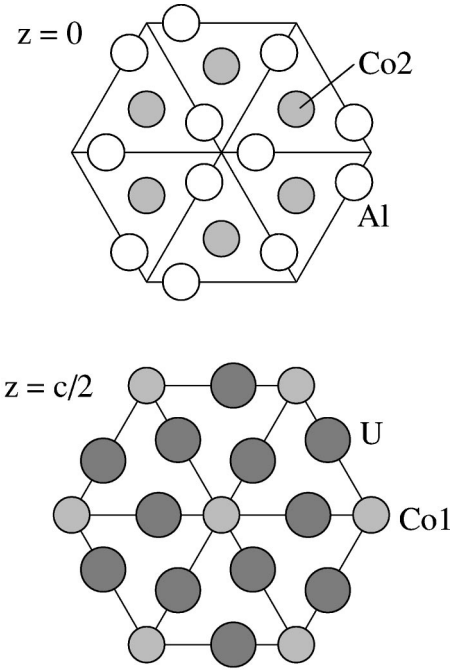

FIG. 1. Schematic picture of the two layers of the ZrNiAl-type crystal structure.

bution throughout the unit cell, especially on the two cobalt sites, and (ii) determine the spin and orbital components of the uranium magnetic moments. In order to understand the microscopic origin of the strong magnetization increase in fields above the metamagnetic transition, we have studied the change of the overall picture in UCoAl when increasing the magnetic field from 1 to 8 T.

II. EXPERIMENT

The UCoAl single crystal has been grown by the Czochralski method in a tetra-arc furnace from the melt of stoichiometric amounts of pure metals (the purity was $3N$ for U, $4N$ for Co, $6N$ for Al). The x-ray diffraction confirmed that the crystal is a single phase with the hexagonal ZrNiAl-type structure. The lattice parameters, determined at room temperature by x-rays, are $a=667.5$ pm and $c=396.6$ pm.[7] The sample used for our neutron-diffraction study has a shape of a flat plate ($4\times0.8\times3$ mm) perpendicular to [100] direction with a length of 3 mm along [001] direction.

Two types of neutron-diffraction experiments have been performed. To refine the nuclear structure parameters at low temperature as well as the extinction parameters of our crystal, integrated intensities of nuclear reflections have been measured on the lifting counter D15 diffractometer at the Institut Laue-Langevin (ILL) Grenoble at 0.851 Å. The crystal was mounted in an orange cryostat with the c axis parallel to the ω axis of the diffractometer and was fixed on a small Al sample holder. The polarized neutron-diffraction experiment has been performed on the D3 diffractometer at the ILL, with an identical sample orientation. The flipping ratios have been measured for $\lambda=0.514$ and 0.843 Å, in magnetic fields of 1 and 8 T applied parallel to the c axis of the UCoAl crystal. The polarization of the incoming neutron beam was 0.8684 (0.8830) and 0.9292 (0.9502) in 1 T (8 T) for $\lambda=0.514$ and 0.843 Å, respectively.

III. CRYSTAL STRUCTURE DETERMINATION

UCoAl crystallizes in the ZrNiAl-type hexagonal structure, a ternary derivative of the Fe_2P structure (space group $P\bar{6}2m$). The structure is a layered one, with U-Co and Al-Co planes alternating along the hexagonal c axis. Both layers are shown in Fig. 1. The atomic positions are following:

$$3\mathrm{U}\ \text{in}\ 3(g):(x,0,\tfrac{1}{2}),\ (0,x,\tfrac{1}{2}),\ (\bar{x},\bar{x},\tfrac{1}{2}),$$

$$3\mathrm{Al}\ \text{in}\ 3(f):\ (y,0,0),\ (0,y,0),\ (\bar{y},\bar{y},0),$$

$$2\mathrm{Co}\ \text{in}\ 2(c):(\tfrac{1}{2},\ \tfrac{2}{3},\ 0),\ (\tfrac{2}{3},\ \tfrac{1}{3},\ 0)$$

(we call this position ''$\mathrm{Co_2}$''),

$1\mathrm{Co}$ in $1(b)$: $(0,\ 0,\ \tfrac{1}{2})$ (we call this position ''$\mathrm{Co_1}$'').

The point-group symmetry at U site is $m2m$. Each U atom has four nearest U neighbors within the U-Co plane at the distance $d_{\mathrm{UU}}=a\sqrt{1-3x+3x^2}\approx346$ pm considering the UCoAl lattice constants given above. The two second nearest U atoms are located along the c axis, at a distance equal to c (= 396.6 pm). The distances between U and Co, generally the U-T distances, are shorter than the U-U ones. The U-T_1 and U-T_2 distances are very similar (281.0 and 281.5 pm, respectively, for UCoAl at 300 K). However, the geometry of the corresponding bonds is quite different: the U-T_1 bonds are located within the U-T plane, whereas U-T_2 bonds point out of this plane.

In order to determine the structure parameters, integrated intensities of 131 nonequivalent (243 total) reflections have been measured at 2 K. The geometry of the experiment (c axis parallel to the ω axis, $\lambda=0.851$ Å) allowed to measure reflections of the $hk0$ and $hk1$ type only. The full-matrix least-square program XFLS was used for the refinement of the crystal structure of UCoAl. The relevant values of the scattering length and the absorption coefficient have been taken.[8,9] Anisotropic temperature factors $b(i,j)$ have been considered. The Becker-Coppens model[10,11] of the secondary extinction correction with the Lorentzian distribution of the angular mosaic block orientation has been applied. In the program, the extinction correction is described by only one parameter g, describing the angular distribution of the mosaic blocks. The contribution from the size of the mosaic blocks has been neglected. The importance of the extinction correction and the reliability of the applied model is demonstrated in Fig. 2. It is clear that this correction is relatively small for our crystal—the largest correction, which is for the 201 reflection, amounted less than 12%. The final results of our refinement are summarized in Table I.

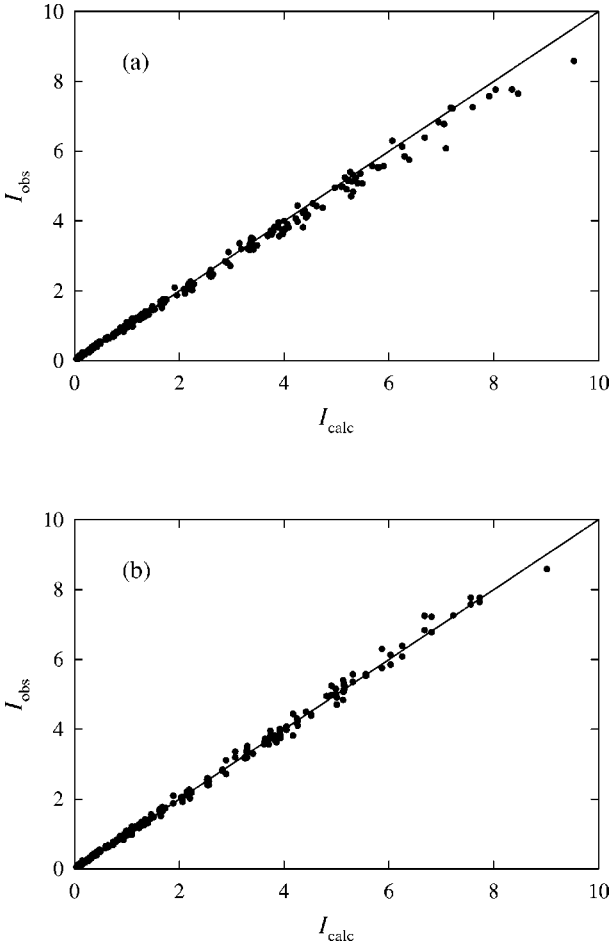

FIG. 2. Plot of I_{obs} vs I_{calc} without (a) and with (b) the extinction correction.

IV. RESULTS OF THE POLARIZED NEUTRON EXPERIMENT

The polarized neutron experiment consists of measuring the peak intensity of Bragg reflections for neutrons polarized parallel and antiparallel to the applied magnetic field. The ratio of these two intensities (corrected for background) gives the value of the so-called flipping ratio R. For a noncentrosymmetric structure, R is given by

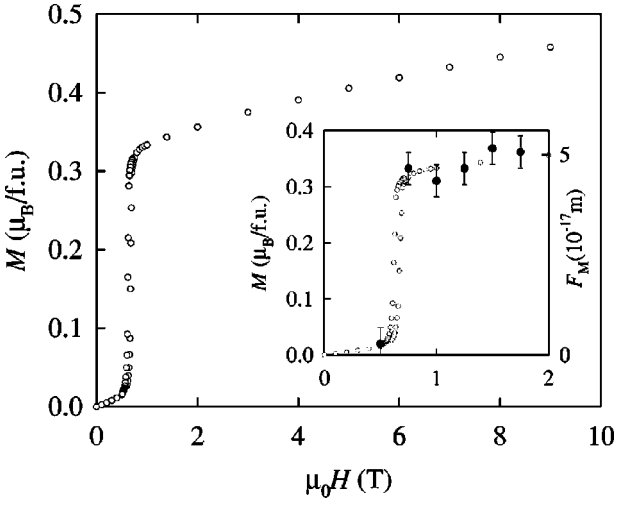

FIG. 3. M vs B data taken from Ref. 7; the inset shows the magnetization data (○) and the values of F_M corresponding to (100) reflection (●).

$$R_{hkl}=\frac{F_N'^2+F_N''^2+2pq^2(F_N'F_M'+F_N''F_M'')+q^2(F_M'^2+F_M''^2)}{F_N'^2+F_N''^2-2pq^2(F_N'F_M'+F_N''F_M'')+q^2(F_M'^2+F_M''^2)}, \tag{1}$$

where F_N and F_M are the nuclear and magnetic structure factors, respectively:

$$F_N=F_N'+iF_N'', \quad F_M=F_M'+iF_M'', \tag{2}$$

p is the polarization of the incident neutron beam and q represents the sine of the angle between the vector of the magnetic structure factor and the scattering vector.

First, we have measured the flipping ratios of the (100) reflection, for which the structure factor is purely real, in a few different applied magnetic fields up to 2 T. Using the structure data (F_N), we obtained the magnetic structure factors F_M, which are displayed in Fig. 3. These data, in agreement with the magnetization measurements, confirm that a magnetic field of 1 T is sufficient to induce the ferromagnetic state in UCoAl.

The main polarized neutron experiment has been performed at $T=2$ K, for applied magnetic fields of 1 and 8 T. The flipping ratios of 63 nonequivalent groups of $hk0$ and

TABLE I. Final refinement of the structural parameters and the extinction correction parameter g for UCoAl at 2 K. $b(i,j)$ are the anisotropic temperature factors; $b(1,2)=b(2,2)/2$, $b(1,3)=b(2,3)=0$ for the hexagonal structure.

Atom type	U	Co_1	Co_2	Al
Position	x, 0, $\frac{1}{2}$	0, 0, $\frac{1}{2}$	$\frac{1}{3}$, $\frac{2}{3}$, 0	y, 0, 0
	$x=0.5788(1)$			$y=0.2358(2)$
Occupation	1	$\frac{1}{3}$	$\frac{2}{3}$	1
$b(1,1)$	0.00064(7)	0.0014(4)	0.0015(3)	0.0015(2)
$b(2,2)$	0.00073(7)	0.0015(4)	0.0015(3)	0.0014(2)
$b(3,3)$	0.0317(10)	0.033(5)	0.046(5)	0.037(3)
$g=0.195(25)$				
R factor$=1.87\%$				

$hk1$ reflections (usually, two equivalent reflections have been measured for each group) with $\sin\theta/\lambda \leq 0.91\ \text{Å}^{-1}$ have been measured at a wavelength of $\lambda = 0.843\ \text{Å}$. To check the extinction correction, 22 strongest nonequivalent reflection groups have been measured also at $\lambda = 0.514\ \text{Å}$. Additionally, at this shorter wavelength, the experimental arrangement enabled us to measure further 23 nonequivalent reflections of the $hk2$ type. No reflection has been excluded from the analysis due to extinction. The same set of reflections has been measured in both fields.

The experimental flipping ratios were analyzed by two different approaches: the maximum entropy method,[12,13] which makes no assumption on the magnetization distribution, and by a classical refinement of an atomic model which considers that the magnetic moments are carried by atomic sites. We consider first the maximum entropy approach.

A. Maximum entropy treatment—spin density maps

The advantage of the maximum entropy method (MAXENT) is that no atomic model is needed for the refinement. The required information is the space-group symmetry, lattice parameters, experimental flipping ratios with corresponding nuclear structure factors, wavelengths, beam path for individual reflections, and the extinction correction parameter g. In our analysis, we have included also the flipping ratios for the (000) reflection, for which F_M is given by the measured bulk magnetization value. For the refinement, we divided the unit cell of UCoAl into $32\times32\times32$ small cells in which the magnetization is assumed to be constant. We started the refinement with a small magnetization having a flat distribution (i.e., the same value in all the cells). As the final result, we have obtained the most probable reconstructed three-dimensional map of the density of the magnetic moment, i.e., the map which fits the data and for which the entropy is maximum.

The best way to show the main features of the three-dimensional map is to make a projection onto the basal plane. The analysis of our data gives a rather good resolution along the c axis that allows us to divide the unit cell into two parts—one containing the U-Co plane, the other one containing Al-Co plane. Each of the two parts contain 16 cells along c. The sufficient resolution has been achieved thanks to the measurement of the $hk2$-type reflections. It is an advantage in comparison to the previous work done on UNiGa and UNiAl,[4] which was restricted to $hk0$ and $hk1$ planes.

The magnetization distributions within the U-Co plane in 1 and 8 T are shown in Fig. 4. The main contribution comes clearly from the uranium atoms. Much weaker magnetization clouds are located on the Co_1 positions. Another way to display the results is to select cell of given coordinates x and y within the basal plane and look at its magnetization variation along the c axis. Such a plot is drawn in Fig. 5 for the central position of U, Co_1, and for the point lying in the middle of the line connecting U and Co_1. The magnetization clouds of U and Co_1 are clearly located in the $z = c/2$ plane. We observe a considerable increase of the magnetization between 1 and 8 T on the uranium site and a decrease on the Co_1 position. This decrease appears just at the center and is overcompensated by an increase in the surrounding area. The total integrated magnetization associated with the Co_1 site thus increases when increasing the field from 1 to 8 T. In addition, a small magnetization arises on the (0, 0, 0) position, where we do not expect any atom. The whole magnetization cloud around this position is rather small (see Fig. 6), and the size of this effect can be understood as accuracy limit of our data and the method.

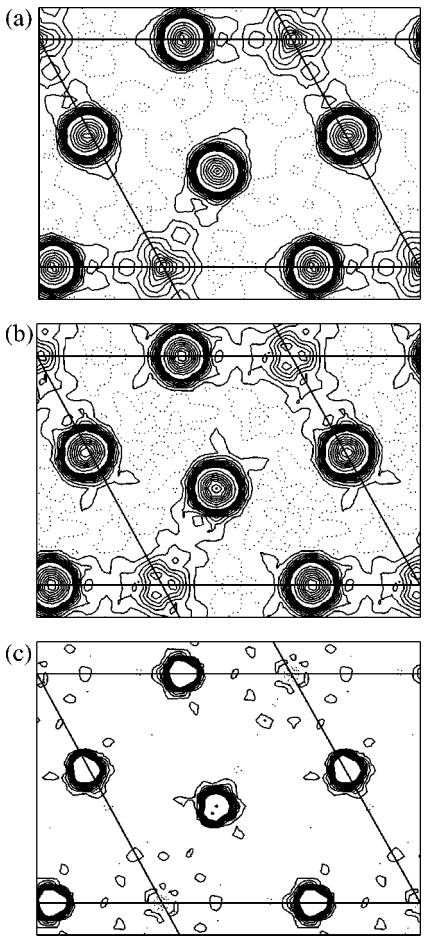

FIG. 4. Density of magnetic moment within the U-Co plane in 1 T (a) and 8 T (b) and differential density ($M_{8T} - M_{1T}$) (c) reconstructed by maximum entropy method. The contours are at $0.01\mu_B/\text{Å}^2$, dotted contours represent negative values. Above $0.1\mu_B/\text{Å}^2$ (center of the uranium position), the contours are at $0.1\mu_B/\text{Å}^2$.

The enhancement of the magnetization distribution on the U sites when the field is increased from 1 to 8 T is slightly anisotropic, as can be better seen on the differential map shown in Fig. 4(c). A small positive magnetization arises in 8 T between U and Co_1 atoms, as seen on Fig. 5. This feature can originate from the polarization of the bonds between uranium and cobalt by applied magnetic field, assuming that d or f electrons participate in the bonding.

In the Al-Co plane, magnetization clouds are observed on the Co_2 positions and close to the Al positions (see Fig. 6). Figure 7 shows clearly that these positive densities are located in the Al-Co plane with a shape similar to that one of the cobalt sites. Magnetic moment induced on aluminum or

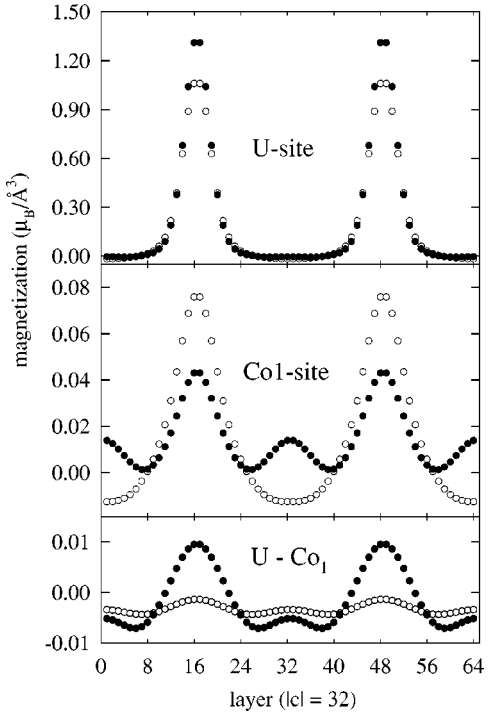

FIG. 5. Density of magnetic moment along the *c* axis in different basal-plane positions; the U-Co_1 means a point on the middle of the line connecting U and Co_1. The white and black symbols represent 1 and 8 T data, respectively.

an atomic disorder between the cobalt and aluminum sublattice, i.e., part of Co atoms is located on the Al sites, could be an explanation. We discuss this possibility later. The magnetization on both the Co_2 and ''Al'' sites increase when increasing the field, as can be seen in Figs. 6 and 7. The increase is again somewhat anisotropic, indicating a possible bond polarization.

The magnetization clouds around all the atomic positions, including aluminum, are sufficiently separated to allow their direct integration. Magnetic moments obtained in this way are given in Table II. A color version of all the density maps is available on www.xray.cz/priv/javor/ucoal.html.

B. Maximum entropy treatment—atomic model

Now, let us consider that magnetic moments are centered on individual atoms with fixed positions. In such a model, the magnetic structure factors are given by the following expression:

$$F_M(Q)=\sum_{\text{at}} G_{\text{at}}(Q)e^{-W_{\text{at}}}\mu_{\text{at}}f_{\text{at}}(Q). \tag{3}$$

Here, the summation goes over all nonequivalent atoms which carry a magnetic moment μ with a corresponding form factor *f*, *Q* is the scattering vector, *W* is the Debye-Waller factor, and *G* is the geometrical factor

$$G(Q)=\sum_j e^{iQr_j}, \tag{4}$$

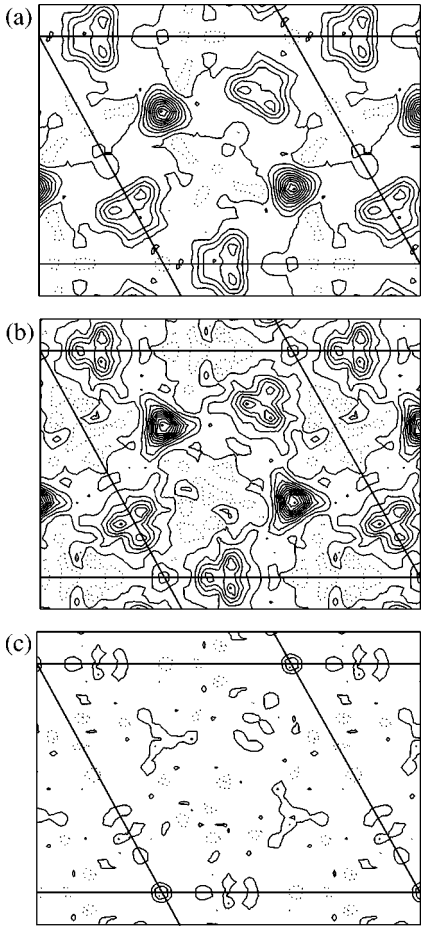

FIG. 6. Density of magnetic moment within the Al-Co plane in 1 T (a) and 8 T (b) and differential density ($M_{8\text{T}}-M_{1\text{T}}$) (c) reconstructed by maximum entropy method. The contours are at $0.01\mu_B/\text{Å}^2$, dotted contours represent negative values.

where we sum over all equivalent positions of a given atom. The geometrical and the Debye-Waller factors can be taken from the nuclear data refinement. For the magnetic form factor of uranium, the dipole approximation is used:

$$\mu_{\text{U}}f_{\text{U}}=\mu_S\langle j_0\rangle+\mu_L(\langle j_0\rangle+\langle j_2\rangle)=\mu(\langle j_0\rangle+C_2\langle j_2\rangle), \tag{5}$$

$$C_2=\frac{\mu_L}{\mu}.$$

The μ_L and μ_S represent the orbital and spin moment of uranium, the $\langle j_n\rangle$ are the radial integrals, tabulated for individual ions.[14] We have considered the both U^{3+} and U^{4+} possibilities. In the case of cobalt, orbital moments are assumed to be negligible, and the form factor is described by $\langle j_0\rangle$ only. We have taken the function corresponding to the Co^{2+} ion.[14]

We fit the magnetic structure factors (real and imaginary part separately) calculated from the reconstructed magnetization maps to Eq. (2). The weights of individual reflections have been taken as

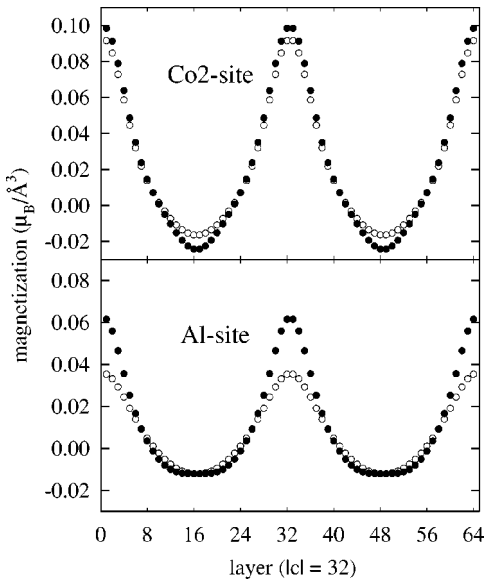

FIG. 7. Density of magnetic moment along the *c* axis in different basal-plane positions; the ''Al'' position means a point close to Al site, where the magnetization reaches local maximum. The white and black symbols represent 1 and 8 T data, respectively.

$$\text{weight}=\left(\frac{1}{\text{err}}\right)^2, \quad \text{err}=\frac{\delta R\cdot R}{R-1}, \tag{6}$$

where R is the flipping ratio calculated from the map and δR the corresponding experimental error for the given reflection. First, we have assumed an uranium magnetic moment on the U site and a cobalt moment on both Co sites. The results are summarized in Table II. A substantial improvement of the fit (the agreement factors improve by a factor of ≈1.6) is achieved assuming additionally cobalt moment on the Al site. It would correspond to the Co-Al atomic disorder. These results are denoted by ''*'' in Table II and represented in Fig. 8. All the results given in Table II have been obtained for $\langle j_n \rangle$ of U^{3+}. Assuming U^{4+}, we have obtained the same values of total moments and the same agreement with the data, and cannot thus make any conclusion about the uranium valence.

C. Flipping ratio direct refinement for an atomic model

Another way to treat the experimental data is the direct refinement of the measured flipping ratios, independently on the maximum entropy results. We assume the magnetic moments on given atomic sites, characterized by magnetic form factors as in the previous treatment. On the U site, we consider two types of moment—one purely orbital, the second purely spin. For the refinement, we have used the Cambridge Crystallography Subroutine Library[14] and refined the experimental data for both wavelengths together. Again, the data are not very sensitive to the uranium valence. In the following, we give the values obtained for U^{3+}. The fit without magnetic moment on the Al site gives an agreement factor of $\chi^2=4.9$ and 8.2 for the data in 1 and 8 T, respectively. Including the cobalt moment on this site, the fit improves seriously: $\chi^2=3.1$ and 4.8 for 1 and 8 T, respectively. The final results are summarized in Table II.

The results obtained by the maximum entropy method and the direct refinement of the flipping ratios are generally in a good agreement, as can be seen in Table II. All the magnetic moments are parallel to the *c* axis (direction of the applied field). The main magnetic contribution comes from the uranium atoms. It increases by ≈25% between 1 and 8 T. The orbital and spin moments are oriented antiparallel and their

TABLE II. Summary of the results obtained by integration in the magnetization density maps, fit of Eq. (1) to the magnetic structure factors calculated from these maps and the direct refinement of the measured flipping ratios; μ_{spd} is obtained by comparing the sum of all moment with the bulk magnetization. By * we denote the results obtained assuming magnetic moment described by cobalt form factor on Al site.

		μ(U) (μ_B/atom)	μ_L (μ_B/atom)	$-\mu_S$ (μ_B/atom)	$-\mu_L/\mu_S$	μ_L/μ	μ(Co$_1$) (μ_B/atom)	μ(Co$_2$) (μ_B/atom)	μ(''Al'') (μ_B/atom)	μ_{spd} (μ_B/f.u.)
1 T	integration in the map	0.326(12)					0.059(11)	0.051(8)	0.048(10)	−0.094
	fit Eq. (1)	0.327(4)	0.602	0.275	2.19	1.84(4)	0.044(4)	0.054(3)		−0.044
	refinement of experimental R	0.300(4)	0.597	0.297	2.01	1.99	0.072(4)	0.049(4)		−0.023
	* fit Eq. (1)	0.341(3)	0.566	0.225	2.52	1.66(3)	0.059(3)	0.049(2)	0.035(2)	−0.094
	* refinement of experimental R	0.317(4)	0.561	0.244	2.30	1.77	0.068(4)	0.046(3)	0.019(3)	−0.055
8 T	integration in the map	0.410(14)					0.068(17)	0.065(8)	0.068(13)	−0.099
	fit Eq. (1)	0.401	0.786	0.385	2.04	1.96(4)	0.039(5)	0.052(4)		−0.004
	refinement of experimental R	0.383(5)	0.785	0.402	1.95	2.05	0.083(6)	0.050(5)		+0.001
	* fit Eq. (1)	0.428(3)	0.728	0.300	2.43	1.70(3)	0.063(3)	0.055(2)	0.049(2)	−0.090
	* refinement of experimental R	0.412(5)	0.733	0.321	2.28	1.78	0.078(4)	0.050(4)	0.029(4)	−0.055

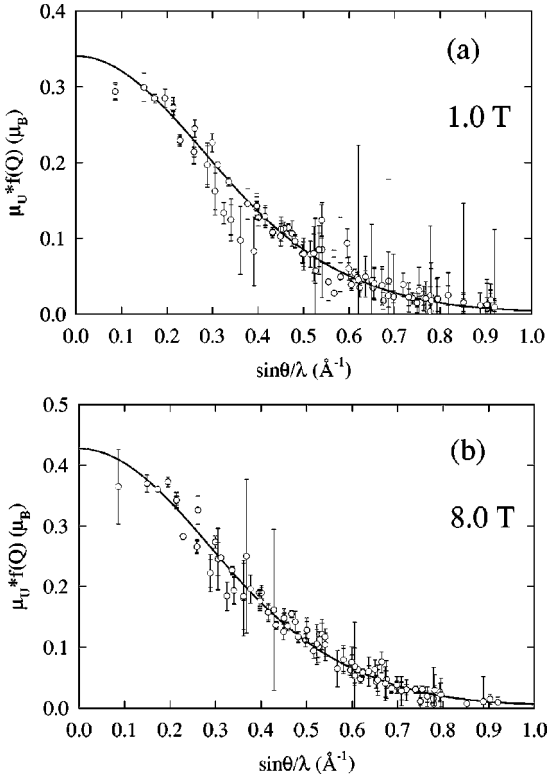

FIG. 8. Form factor curve of UCoAl in 1 T (a) and 8 T (b); the points represent values calculated from the reconstructed density maps after subtraction of the cobalt contribution, the lines represent the form factor calculated by Eq. (3) using the parameters given in Table II.

ratio remains nearly unchanged by increasing the magnetic field. The induced magnetic moment on cobalt positions is about $0.05\mu_B$. It is somewhat larger on Co_1 than on Co_2. The additional moments around the Al site are larger when integrating the reconstructed maps. The integration involves all the space, while in the refinement of the atomic model, we consider moments on given fixed positions only. In case of the Co-Al atomic disorder, the Co atoms could be located not exactly on the Al site, but distributed around it. Such disorder is not considered in the atomic model while the integration includes it.

Comparing the total sum of all the moments with the bulk magnetization value,[7] one can infer the residual conduction electron polarization μ_{spd}. This moment is in total oriented parallel to the uranium spin moment [antiparallel to the total μ(U)].

V. DISCUSSION

Our study reveals rather clearly an existence of magnetization distribution around the Al sites. A similar effect has been observed in UNiGa and UNiAl.[4] Due to poor resolution along the *c* axis, it was not possible to locate these clouds in that study. Our resolution is better, and as shown in Fig. 7, these positive densities are located in the Al-Co plane and have a shape similar to that of cobalt sites. The corresponding magnetic moment is oriented parallel to the total uranium moment. We have tentatively ascribed this effect to the Co-Al atomic disorder. A similar explanation has been considered also for UNiGa and UNiAl (Ref. 4) (i.e., Ni-Ga or Ni-Al disorder). The magnitude of the moment located on Al sites is well comparable to that on Co sites. That would mean either a large degree of disorder (e.g., 50% of Co atoms on Al sites) or rather large moment carried by the Co atoms on the Al sites (e.g., 10% disorder would mean almost $0.5\mu_B$ per such Co atom). The latter possibility does not seem to be realistic. A question then arises, whether the large degree of Co-Al disorder would be observed when determining crystal structure. In the case of x-ray diffraction, most of the intensity is due to the scattering on the uranium and the mentioned disorder would have almost negligible influence on the reflection intensities. For the neutron diffraction, the scattering length of Co (2.5 fm) and Al (3.4 fm) do not differ substantially and are much smaller than that of U (8.4 fm).[8] The disorder would be thus relatively hardly observable. A somewhat more favorable situation exists for UNiGa and UNiAl. The scattering length of Ni [10.3 fm (Ref. 8)] is large compared especially to that of Al. However, no strong evidence for a large Ni-Ga or Ni-Al disorder has been found in the crystal structure refinement of UNiGa and UNiAl.[4] The origin of these magnetization distributions around Al site, which are clearly above the experimental error, remains questionable.

Let us now turn to the uranium magnetic moment. The ratio $-\mu_L/\mu_S$ determined from our data (see Table II) is reduced compared to the U^{3+} free ion value of 2.57, but the reduction is smaller than in the isostructural UNiGa ($-\mu_L/\mu_S=1.98$), UNiAl ($-\mu_L/\mu_S=1.79$), or URhAl ($-\mu_L/\mu_S=1.81$). The large orbital contribution is remarkable for a material such as UCoAl, which is considered as one of the U*TX* compounds with rather delocalized $5f$ electrons.[1] We shall note that both μ_L and μ_S are strongly reduced with respect to the corresponding free ion values. The values of the spin and orbital moments have been derived also in Ref. 5, based, however, on analysis of 11 centrosymmetric reflections only. The data obtained earlier in 1.7 T are similar to our results in 1 T. An increase of μ_L and unchanged μ_S have been reported in a field of 5 T. Our data reveal a different development when increasing the magnetic field: both μ_L and μ_S increase and their ratio remains almost unchanged (see Table II).

Another highly interesting question is connected with the anisotropy of the hybridization between the uranium $5f$ states and transition-metal *d* states. As mentioned in the introduction, a large anisotropy has been observed for URhAl and URuAl. Our study does not show any indication for such a large hybridization anisotropy in UCoAl, and confirms the previous experiment. The following values for the cobalt moments induced in a field of 5 T have been reported in the former study: $\mu(Co_1)=0.058\mu_B$, $\mu(Co_2)=0.076\mu_B$.[6] The $\mu(Co_2)$ moment increases with the field, whereas $\mu(Co_1)$ has been reported as insensitive to the applied field. In contrast, our analysis shows that the moment on Co_1 is slightly larger than that on Co_2 and both moments increase when increasing the magnetic field by $\approx$10–20% between 1 and 8 T (see Table II). The magnitude of the magnetic moments

induced on cobalt is about 20% of the uranium moments, less than in URhAl (30%) or URuAl (45%). This is expected because the $4d$ wave functions of Rh or Ru are more expanded in space than the $3d$ states of Co, which leads to stronger hybridization in the $4d$ compounds. The $5f$-$3d$ hybridization in UCoAl is apparently stronger than in UNiAl or UNiGa (the Ni moments are about 10% of U moments) since the cobalt $3d$ states are in lower binding energies (i.e., closer to E_F) than the nickel $3d$ states.[15] The increase of the cobalt moment induced by the field is smaller compared to the uranium moment. This could be an indication of a weakening of the hybridization.

Comparing the results obtained by polarized neutron diffraction for URhAl, URuAl, UNiAl, UNiGa, and UCoAl, one could speculate that the hybridization is strongly anisotropic (occurs mainly within the U-T plane) for the $4d$ series, while no such strong anisotropy appears for the $3d$ series. The U-T_1 and U-T_2 distances are very close to each other in all the mentioned compounds, and cannot thus serve as an explanation for such a different behavior. The nature of the d states plays probably the crucial role. In this context, it would be highly interesting to investigate an isostructural UTX compound from the $5d$ series, e.g., UPtAl which is a simple ferromagnet with uranium moments aligned along the c axis.[1,16]

VI. CONCLUSIONS

Our polarized neutron data confirm that the main magnetic contribution in UCoAl comes from the uranium atoms. The ratio between the orbital and spin moment is slightly reduced in comparison to the U^{3+} free ion value, but the reduction is smaller than in other isostructural UTX compounds. It remains nearly unchanged between 1 and 8 T. Both μ_L and μ_S are very reduced compared to the corresponding free ion values. We have observed induced magnetic moments of comparable magnitude and similar field dependence on both cobalt sites. An additional magnetization is observed around the aluminum positions.

ACKNOWLEDGMENTS

We acknowledge the kind assistance of P. J. Brown who modified her program MAGLSQ included in the Cambridge Crystallography Library, in order to refine together the data corresponding to different wavelengths. We acknowledge also the support from ILL technical services. The work was supported by the Grant Agency of the Czech Republic (Grant Nos. 202/98/P245 and 202/99/0184).

*Corresponding author. Fax: +420 2 2191 1351. Email address: javor@mag.mff.cuni.cz

[1] V. Sechovský and L. Havela, in *Handbook of Magnetic Materials*, edited by K. H. J. Buschow (Elsevier Science B. V., Amsterdam, 1998), and references therein.
[2] J. A. Paixão, G. H. Lander, P. J. Brown, H. Nakotte, F. R. de Boer, and E. Brück, J. Phys.: Condens. Matter **4**, 829 (1992).
[3] J. A. Paixão, G. H. Lander, A. Delapalme, H. Nakotte, F. R. de Boer, and E. Brück, Europhys. Lett. **24**, 607 (1993).
[4] M. Olšovec, J. Schweizer, L. Paolasini, V. Sechovský, and K. Prokeš, Physica B **241–243**, 678 (1998); M. Olšovec, Ph.D. thesis, Prague, 1999.
[5] M. Wulff, J. M. Fournier, A. Delapalme, B. Gillon, V. Sechovský, L. Havela, and A. V. Andreev, Physica B **163**, 331 (1990).
[6] R. J. Papoular and A. Delapalme, Phys. Rev. Lett. **72**, 1486 (1994).
[7] N. V. Mushnikov, T. Goto, K. Kamishima, H. Yamada, A. V. Andreev, Y. Shiokawa, A. Iwao, and V. Sechovský, Phys. Rev. B **59**, 6877 (1999).
[8] V. F. Sears, Neutron News **3**, 26 (1992).
[9] V. McLane, Ch. L. Dunford, and P. F. Rose, *Neutron Cross Sections* (Academic, New York, 1984).
[10] P. J. Becker and P. Coppens, Acta Crystallogr., Sect. A: Cryst. Phys., Diffr., Theor. Gen. Crystallogr. **30**, 148 (1974).
[11] P. J. Becker and P. Coppens, Acta Crystallogr., Sect. A: Cryst. Phys., Diffr., Theor. Gen. Crystallogr. **30**, 129 (1974).
[12] R. Papoular and B. Gillon, Europhys. Lett. **13**, 379 (1990).
[13] P. Schleger, A. Puig-Molina, E. Ressouche, O. Rutty, and J. Schweizer, Acta Crystallogr., Sect. A: Found. Crystallogr. **53**, 426 (1997).
[14] P. J. Brown and J. C. Matthewman, *The Cambridge Crystallography Subroutine Library, Mark 4 User's Manual*, Rutherford Appleton Laboratory Report, 1993.
[15] T. Gasche, M. S. S. Brooks, and B. Johansson, J. Phys.: Condens. Matter **7**, 9499 (1995).
[16] A. V. Andreev, Y. Shiokawa, M. Tomida, Y. Homma, V. Sechovský, N. V. Mushnikov, and T. Goto, J. Phys. Soc. Jpn. **68**, 2426 (1999).